Acta Pharmaceutica Sinica B 2023;13(2):648–661

Chinese Pharmaceutical Association
Institute of Materia Medica, Chinese Academy of Medical Sciences

Acta Pharmaceutica Sinica B

www.elsevier.com/locate/apsb
www.sciencedirect.com

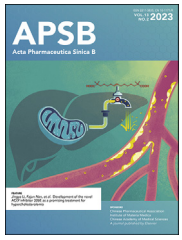

ORIGINAL ARTICLE

The role of CYP1A1/2 in cholesterol ester accumulation provides a new perspective for the treatment of hypercholesterolemia

Jian Lu[†], **Xuyang Shang**[†], **Bingyi Yao**[†], **Dongyi Sun, Jie Liu, Yuanjin Zhang, He Wang, Jingru Shi, Huaqing Chen, Tieliu Shi, Mingyao Liu, Xin Wang**[*]

Changning Maternity and Infant Health Hospital and School of Life Sciences, Shanghai Key Laboratory of Regulatory Biology, East China Normal University, Shanghai 200241, China

Received 17 March 2022; received in revised form 30 June 2022; accepted 18 July 2022

KEY WORDS

Hyperlipidemia;
Hypercholesteremia;
Cholesterol;
CYP1A;
Lipidosis;
LXR;
CES1;
Lansoprazole

Abstract Cholesterol is an important precursor of many endogenous molecules. Disruption of cholesterol homeostasis can cause many pathological changes, leading to liver and cardiovascular diseases. CYP1A is widely involved in cholesterol metabolic network, but its exact function has not been fully elucidated. Here, we aim to explore how CYP1A regulates cholesterol homeostasis. Our data showed that *CYP1A1/2* knockout (KO) rats presented cholesterol deposition in blood and liver. The serum levels of low-density lipoprotein cholesterol, high-density lipoprotein cholesterol and total cholesterol were significantly increased in KO rats. Further studies found that the lipogenesis pathway (LXRα−SREBP1−SCD1) of KO rats was activated, and the key protein of cholesterol ester hydrolysis (CES1) was inhibited. Importantly, lansoprazole can significantly alleviate rat hepatic lipid deposition in hypercholesterolemia models by inducing CYP1A. Our findings reveal the role of CYP1A as a potential regulator of cholesterol homeostasis and provide a new perspective for the treatment of hypercholesterolemia.

*Corresponding author.
E-mail addresses: xwang@bio.ecnu.edu.cn, usxinwang@gmail.com (Xin Wang).
[†]These authors made equal contributions to this work.

Peer review under the responsibility of Chinese Pharmaceutical Association and Institute of Materia Medica, Chinese Academy of Medical Sciences.

https://doi.org/10.1016/j.apsb.2022.08.005

1. Introduction

Hyperlipidemia refers to dyslipidemia, which is characterized by elevated triglyceride (TG), total cholesterol (T-C), low density lipoprotein cholesterol (LDL-C) and decreased high density lipoprotein cholesterol (HDL-C) in blood[1,2]. In particular, high cholesterol in the blood is defined as hypercholesterolemia[3]. Cholesterol is an essential component of vertebrate cell membrane, which is essential to maintain its structure and function[4]. Cholesterol and its metabolites, such as steroid hormones, oxysterols and bile salts, possess important biological functions[5]. Therefore, the regulation of cholesterol homeostasis is of great significance to the physiological and pathological status of the body. Cholesterol homeostasis plays a remarkable role in balancing blood lipid levels, and high levels of LDL-C are associated with high risk of cardiovascular disease (CVD)[6]. CVD is the primary cause of death among adults in the United States, and people with hyperlipidemia exposure for 11−20 years have about four times the risk of CVD as those who have not been exposed[7]. At the same time, about 53% of adults in the United States have been detected the elevated LDL-C level[8]. In China, CVD is also the main cause of death and premature death, accounting for 40% of the death population[9].

The main source of cholesterol in human body includes the absorption from food and bile, and the newly synthesized cholesterol. In humans and experimental animals, there are two main ways to remove cholesterol, that is, to secrete bile cholesterol through the tubular membrane of hepatocytes and to metabolize cholesterol into other metabolites. Liver is the main organ to maintain cholesterol homeostasis, and is considered to be the main site for cholesterol biotransformation[10,11]. Cholesterol can be synthesized by acetate with the intermediate of lanosterol. On the contrary, cholesterol can be converted to cholic acid through classical and alternative pathways in the liver, which are activated by CYP7A1 and CYP27A1, respectively[12]. Although CYP1A does not directly participate in the metabolism of cholesterol, it is widely involved in the metabolic network that converts cholesterol into hormones[11]. The effects of CYP7A1[13,14] and CYP27A1[15,16] on cholesterol metabolism have been extensively explored, but the cholesterol metabolism mediated by CYP1A and its physiological effects have not been systematically reported. As an important member of CYP superfamily, CYP1A is not only involved in the metabolism of nearly 9% clinical drugs, but also participates in the transformation of endogenous substances, such as all-*trans*-retinoic acid, prostaglandin G_2, oestrogen, uroporphyrinogen, and melatonin[11,17,18], which affect the homeostasis of these endogenous molecules. Thus, the metabolic abnormality of CYP1A in endogenous molecules may lead to physiological or pathological changes. Since 1990s, the physiological or pathological functions of CYP1A have been preliminarily studied[19−21].

Although CYP1A is involved in lipid homeostasis, its specific function remains unclear. Therefore, in order to understand the important role of CYP1A in lipid-related metabolic diseases, we constructed a new *CYP1A1/2* double knockout (KO) rat model. The phenotypes of hypercholesteremia and hepatic cholesterol deposition were observed. Further studies confirmed that the expression of CES1 decreased and the LXRα−SREBP1−SCD1 pathway was activated in *CYP1A1/2* KO rats. More importantly, we found that CYP1A inducer can effectively reduce blood cholesterol ester levels and hepatic cholesterol deposition. Overall, our findings provide evidence for the role of CYP1A in cholesterol homeostasis, and provide a new perspective for the treatment of hypercholesterolemia.

2. Methods and materials

2.1. Chemicals and supplies

Oligos (60 bp, containing sequences of *CYP1A1* and *CYP1A2* target sites) and all primer pairs for PCR were synthesized by Biosune Biotechnology Co., Ltd. (Shanghai, China). SYBR Premix Ex Taq and Prime Script RT Reagent Kit were bought from Takara (Dalian, China). Primary antibodies for CYP1A1/2 (ab22717), LXRα (ab176323), CES1 (ab45957) and GAPDH (ab181602) were purchased from Abcam (Cambridge, UK). Primary antibodies for SCD1 (sc-58420) and SREBP1 (sc-365,513) were supplied by Santa Cruz (Heidelberg, Germany). Primary antibody for CES2 (BS5659) was supplied by Bioworld technology, Co., Ltd. (Nanjing, China). The fluorescence-conjugated secondary antibody to rabbit IgG and mouse IgG were purchased from Cell Signaling Technology (Boston, USA). Lansoprazole (Lan) was purchased from Energy Chemical (Shanghai, China). Cholesterol rich diet (D12108C, cholesterol content 1.25%) was bought from Research Diet (New Brunswick, USA). The ELISA kit for pregnenolone detection was purchased from Novus biological (Centennial, USA). Free cholesterol detection kit was bought from Beijing Solarbio Science & Technology Co., Ltd. (Beijing, China).

2.2. Animals and treatment

Male and female Sprague−Dawley rats were purchased from National Rodent Laboratory Animal Resources (Shanghai, China). Rats were housed in the specific pathogen free environment with a relative humidity of 55% and temperature at 22 °C, with 12 h light/dark cycles. All animals were kept with free access to sterile water and standard rodent food. The project was conducted in accordance with the Helsinki Declaration and the National Institutes of Health Guide for the Care and Use of Laboratory Animals. All experiments were conducted under permission of Ethics Committee on Animal Experimentation of the East China Normal University (Shanghai, China).

The *Ldlr* KO rats (8-week-old male rats) were randomly divided into two groups with 6 rats in each group. All rats were kept with free access to sterile water and standard rodent food. The experimental group ($LDLR^{-/-}$ + Lan 50 group) was treated with Lan (50 mg/kg/day, *p.o.*) for 21 days, and the control group ($LDLR^{-/-}$ + Sol group) was given the same amount of solvent. Immediately after euthanasia, serum samples were collected and liver tissue was separated for further use.

For the food-borne hyperlipidemia model, wild type (WT) rats were randomly divided into four groups with 6 rats in each group. The low-cholesterol diet group (LCD + Sol group) was fed with standard rodent food and treated with equal volume of solvent. The high-cholesterol diet group (HCD + Sol group) was fed with cholesterol rich diet and treated with the same amount of solvent. Rats in Lan treatment group were fed with cholesterol rich diet and treated with low dose (10 mg/kg/day, HCD + Lan 10 group) or high dose (50 mg/kg/day, HCD + Lan 50 group) of Lan for 11 weeks. Serum samples were collected immediately after euthanasia, and liver tissue was separated for further use.

2.3. Target-site selection

For the selection of target sites, sequences of *CYP1A1* and *CYP1A2* were analyzed. Sequences were submitted to an online

optimized CRISPR design tool (http://tools.genome-engineering.org) to obtain potential target information. Selected target sites of *CYP1A1* and *CYP1A2* were DNA sequences (18 bp) with a PAM site (5′-NGG-3′) in the 3′ end.

2.4. *In vitro construction of single guide RNA (sgRNA) and Cas9 mRNA*

Firstly, a 60 bp oligo DNA sequence containing T7 promotor and 18 bp target sequence was synthesized *in vitro*, and cloned into the pGS3-T7-gRNA vector by overlapping PCR procedure to get sgRNA transcription templates. Then, using the oligo DNA sequence as template, the DNA sequence of sgRNA was obtained by PCR with universal primer *in vitro*. Finally, sgRNA was constructed by *in vitro* transcription using T7 transcription Kit, followed by purification with phenol/chloroform extraction. Cas9 expression vector was linearized by Not I and purified by phenol/chloroform extraction, and then transcribed to mRNA according to the instruction of mMessage mMachine SP6 kit.

2.5. *Microinjection of sgRNA and Cas9 mRNA into zygote*

Rat preparation and microinjection were performed as previously described[22]. In brief, the *CYP1A1* sgRNA (25 ng/μL), *CYP1A2* sgRNA (25 ng/μL) and Cas9 mRNA (50 ng/μL) with buffer were injected into the cytoplasm of one-cell embryos. After overnight incubation in the incubator, the injected zygotes were transplanted into the oviduct of the pseudopregnant female rats.

2.6. *Genotyping of founders and progenies*

Genomic DNA was extracted on 7−10 days after birth. The purified DNA was amplified using the primer pairs for *CYP1A1* and *CYP1A2* listed in Supporting Information Table S1. To identify the genotyping of F_0 generation, T7 endonuclease I (T7EI) assay was used to screen insertion and deletion mutations in the genes. To further determine the modification details, the PCR product of each rat was cloned to pMD-18T vector for sequencing. For the genotyping of F_1 and F_2, the genomic DNA was extracted and PCR products were sequenced directly. The sequencing results were analyzed by DNAMAN (LynnonBiosof, CA, USA).

2.7. *Off-target effects evaluation*

The off-target information was obtained from the off-target searching website (http://cas9.wicp.net/) after the target sequence was input. Off-target sites with a score more than 3.0 were selected to analyze whether there were mutations in these sites using T7EI assay. The primers used in the off-target analysis were listed in Supporting Information Table S2.

2.8. *Metabolic capacity evaluation of CYP1A in CYP1A1/2 KO rats in vitro*

The preparation protocol of rat liver microsomes (RLM) was modified according to our previous study[23]. Caffeine was selected as the probe substrate to monitor the metabolic activity of CYP1A in rats[24]. The incubation mixture includes the NADPH regenerating system (0.4 U/mL glucose 6-phosphate dehydrogenase, 5 mmol/L glucose 6-phosphate, and 1 mmol/L NADP), caffeine (20−1000 μmol/L), and 1 mg/mL of RLM in 0.05 mol/L Tris−HCl buffer (pH 7.4). The incubation was stopped by adding 20 μL of precooled perchloric acid (1.8 mol/L) after incubation for 60 min. The caffeine and its metabolites were analyzed by LC−MS/MS. The Michaelis constant (K_m) and maximum velocity (V_{max}) were analyzed by GraphPad Prism 8.0 (GraphPad Software Inc., San Diego, CA, USA), and the ratio of V_{max}/K_m was defined as intrinsic clearance (CL_{int}).

2.9. *Pharmacokinetic study of caffeine*

The 8-week-old male WT and *CYP1A1/2* KO rats (five rats for each group) were given caffeine (5 mg/kg) by gavage to compare the difference in the pharmacokinetic behavior of caffeine between the two groups. Blood samples were collected from the tail into heparinized centrifuge tubes at 15, 30, 60, 90, 120, 18, 240, 360, 480, and 720 min after administration. Then the whole blood was centrifuged at 6000×*g* for 15 min at 4 °C. The obtained plasma was stored by freezing at −20 °C until further LC−MS/MS detection.

2.10. *Analysis of serum physiological indexes*

The 8-week-old male *CYP1A1/2* double KO rats and WT rats were used to determine whether there were physiological abnormalities in *CYP1A1/2* KO rats. The serum of rat in each group was collected. The collected serum samples were sent to ADICON Clinical Laboratories (Shanghai, China) for the hematological analysis. The detected serum physiological indexes include albumin (ALB), globulin (GLB), total protein (TP), alkaline phosphatase (AP), alanine aminotransferase (ALT), aspartate aminotransferase (AST), direct bilirubin (D-BIL), indirect bilirubin (ID-BIL), total bilirubin (T-BIL), total bile acid (TBA), TG, LDL-C, HLD-C and T-C.

2.11. *Histopathological analysis*

Rat liver samples were fixed in 4% paraformaldehyde at 4 °C overnight. For hematoxylin and eosin (HE) staining, the tissue was embedded in paraffin, sectioned, and stained with HE. For oil red O staining, the tissue was embedded in 'optimal cutting temperature compound' at −20 °C, sectioned and stained with oil red O.

2.12. *Measurement of lipids in liver*

Liver tissue was homogenized with methanol (300 μL/100 mg tissue), followed by extracting lipids with chloroform (600 μL/100 mg tissue) at 4 °C for 12 h. The mixture was centrifuged under the conditions of 4 °C, 12,000 × *g* for 20 min. The supernatant was transferred to a new centrifuge tube and the liquid was dried under the atmosphere of nitrogen. The precipitation was reconstituted with alcohol and the extracted lipids were detected by ADICON Clinical Laboratories.

2.13. *Pregnenolone detection*

The concentration of pregnenolone was determined by ELISA kit. The operation procedure was carried out according to the product manual.

2.14. *Reverse transcription quantitative polymerase chain reaction (RT-qPCR)*

The 8-week-old male rats were sacrificed and tissues were isolated. For the extraction of total RNA, tissues were ground to homogenate with 1 mL Trizol using tissue homogenizer. The total RNA was reverse transcribed into cDNA using Takara RR036A RT kit according to the manufacturer's instructions. SYBR-PCR was performed on Quant Studio 3 Real-Time PCR System (Thermo Fisher Scientific, USA) with SYBR Premix Ex Taq. Primers for RT-qPCR were listed in Supporting Information Table S3. The relative mRNA expression was measured by normalized to the expression of β-actin.

2.15. *Western blot analysis*

Male *CYP1A1/2* KO rats and WT rats were executed and liver was isolated and stored at −80 °C until analysis. Total protein was extracted by RIPA (500 μL/100 mg tissue) containing protease inhibitor, phosphatase inhibitor and PMSF following liver ground to homogenate. Protein sample (40 μg) was loaded onto 10% SDS-PAGE and then transferred onto nitrocellulose membrane. The nitrocellulose membrane was then incubated with anti-CYP1A, anti-Ces1, anti-LXRα, anti-SREBP1 and anti-Scd1 primary antibody overnight at 4 °C. After incubation with secondary antibodies to rabbit IgG or mouse IgG, the results were obtained using Odyssey CLx.

2.16. *Free cholesterol detection*

The free cholesterol concentrations in serum, liver, bile, urine, and faeces were detected according to the instruction manual. Free cholesterol in liver and faeces were extracted using isopropanol (1 mL isopropanol per 100 mg liver or faeces). Working solution was added into 96-well plates (190 μL/well) and then samples (including standard sample) were added into wells (10 μL/well). The mixture was incubated at room temperature for 15 min, and then the absorbance was detected at 500 nm. The concentration of free cholesterol in samples was calculated by the single-point external standard method.

2.17. *Bile acid quantification*

The detection of bile acid was conducted by using an Excel C18-AR chromatographic column (1.7 μm, 2 mm × 100 mm, ACE, UK) and the mobile phase contained water-ACN (containing 0.01% formic acid, *v*/*v*). The bile acid was extracted from rat liver and faeces by using ethyl acetate. For the detection of bile acid in rat serum, liver, bile, urine and faeces, 50 μL of sample was mixed with 150 μL ACN containing internal standard (100 ng/mL chlorpropamide). The mixture was centrifuged at 16,900 × *g* for 20 min after vortex. The supernatant was transferred to a 96-well plate for LC−MS/MS analysis.

2.18. *Statistical analysis*

All data were presented as mean ± standard deviation (SD). Statistical analysis between two groups was performed using unpaired two-tailed *t*-test, and one-way ANOVA was used for multiple groups. The P-value < 0.05 was considered statistically significant. Pharmacokinetic parameters were calculated by WinNonlin software version 5.2.1 (Pharsight Corporation, Mountain View, USA) based on non-compartmental analysis.

3. Results

3.1. *CYP1A1/2 gene KO rat model was successfully constructed by CRISPR/Cas9*

The schematic diagram of target design is presented in Fig. 1A. For targeting *CYP1A1* and *CYP1A2* in the rat, 5′-TCTGCCTTGGATTCTGGG-3′ followed with TGG and 5′-CTGGGGCTTGCCCTTCAT-3′ followed by AGG were selected as the target-sites, respectively. All templates for sgRNA transcription along with the sgRNA and Cas9 mRNA were qualified through agarose gel electrophoresis (Supporting Information Fig. S1).

After co-microinjection of sgRNA and Cas9 mRNA into fertilized eggs of rats, four cubs were born. The targeted loci of *CYP1A1/2* were amplified, and T7EI assay was applied to detect the modifications of genes. The T7EI digestion results showed that all of four cubs were detected with cleavages in the *CYP1A1* targeted loci, and three cubs (F_0-1#, 3#, 4#) were detected with cleavages in the *CYP1A2* targeted loci (Fig. 1B). Then the PCR products were sequenced to detect the mutation details of F_0 founders. For *CYP1A1*, F_0-1#, 4# and for *CYP1A2*, F_0-1#, 3#, 4# contained at least one frameshift mutation. Thus, F_0-1# and 4# were crossed with WT rats to generate heterozygotes with mutations at both targeted loci. Finally, double KO homozygotes with 1 bp insertion of *CYP1A1* and 4 bp deletion of *CYP1A2* at both gene loci were obtained (Supporting Information Figs. S2 and S3A). To evaluate off-target effects of the two sgRNAs, we detected ten and four off-target sites for *CYP1A1* and *CYP1A2* sgRNA, respectively. The results show that no off-target effect was detected at all the selected potential off-target sites (Fig. S3B and S3C). By Western blot analysis, no specific band of CYP1A was observed in the liver of *CYP1A1/2* KO rats (Fig. 1C).

3.2. *CYP1A1/2 deficiency decreased its metabolic function*

Caffeine was used to evaluate the metabolic capacity of *CYP1A1/2* KO rats, and the metabolic activity of RLM from KO rats significantly decreased (Fig. 1D). The K_m remained unchanged between WT and KO groups (Fig. 1E), but compared with the WT rats, the V_{max} of 3-demethylation caffeine formation in KO rats decreased by 38%, and the CL_{int} of caffeine decreased by 50% (Fig. 1F and G). Pharmacokinetic results demonstrate that *CYP1A1/2* deficiency significantly increased the area under curve (AUC) of caffeine by 200% and decreased the AUC of paraxanthine (metabolite of caffeine) by 92%, compared with the WT group (Fig. 1H and I, Supporting Information Tables S4 and S5).

3.3. *CYP1A1/2 deficiency promoted cholesteryl ester accumulation*

To investigate the effects of CYP1A deficiency on the physiology of rats, serum samples were taken at 8 weeks to detect serum protein (ALB, GLB, ALB/GLB, and TP), AP, transaminase (AST, ALT, and AST/ALT), bilirubin (D-BIL, ID-BIL, and T-BIL), TBA and serum lipids (TG, LDL-C, HDL-C, T-C, and HDL-C/LDL-C). Except for serum lipids, most of endogenous substances mentioned above remained unchanged in KO rats

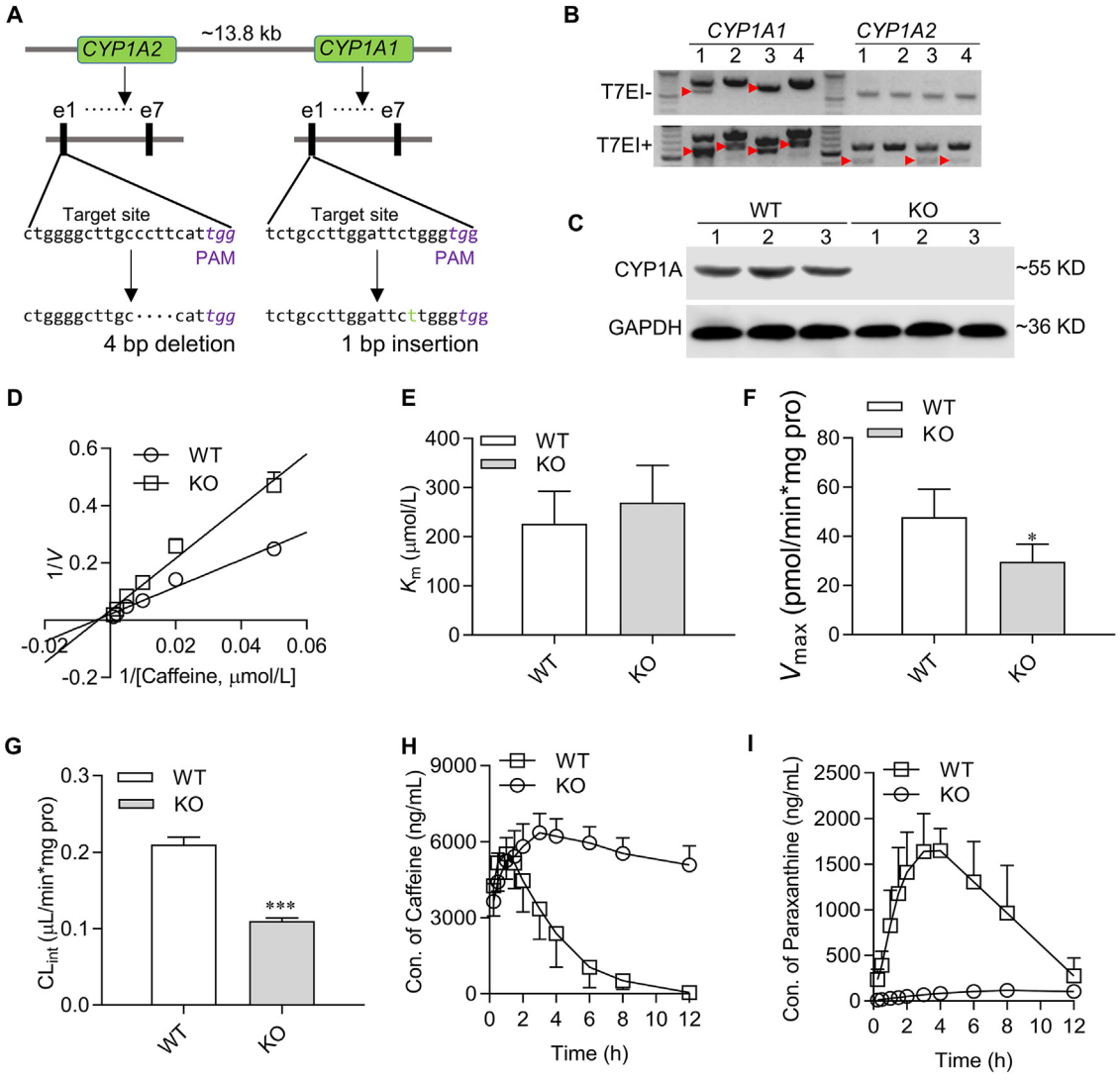

Figure 1 *CYP1A1/2* gene KO rat model was successfully constructed by CRISPR/Cas9. (A) The strategy for the generation of *CYP1A1/2* double KO rat model. (B) Detection of mutations in the F_0 generation through T7EI digestion. T7EI−, before T7EI digestion. T7EI+, after T7EI digestion. Arrow, mutant band. (C) The protein expression of CYP1A in the KO rat. (D) Lineweaver−Burk plot of 1/*V versus* 1/[Caffeine] for the reaction catalyzed by CYP1A in the RLM of WT and KO rats. (E) The K_m of caffeine metabolism in RLM from WT and KO rats. (F) The V_{max} of caffeine metabolism in RLM from WT and KO rats. (G) The CL_{int} of caffeine metabolism in RLM from WT and KO rats. (H) The pharmacokinetic profiles of caffeine in WT and KO rats. (I) The concentration−time curve of caffeine metabolite paraxanthine in WT and KO rats. All data are expressed as mean ± SD, $n = 4$ in (D)−(G), and $n = 6$ in (H)−(I). $^*P < 0.05$, $^{***}P < 0.001$, compared with data in the WT group.

(Fig. 2A). In the serum of *CYP1A1/2* KO rats, LDL-C, HDL-C and T-C levels were up-regulated by about 50%, while the TG concentration was reduced by 17% (Fig. 2B). In addition, the concentrations of free cholesterol in serum and liver of KO rats increased significantly, while those in bile and urine decreased significantly (Fig. 2C).

To further clarify the effect of *CYP1A1/2* deficiency on the liver lipid content, liver slices were stained with HE and oil red O, respectively. HE staining showed that the deletion of *CYP1A1/2* increased the lipid droplets in the liver slice of rats, and oil red O staining showed more reddish liver in the *CYP1A1/2* KO rat (Fig. 2D and E). Lipids were extracted from liver tissues and then the content of lipids was analyzed. Results show that LDL-C, HDL-C, and T-C in the liver of KO rats increased, while the TG concentration remained unchanged (Fig. 2F). In addition to cholesterol, pregnenolone, an important intermediate in cholesterol metabolism, was also accumulated in the blood of KO rats, and its content was three times more than that of WT rats (Fig. 2G). These findings show that lipid deposition, especially cholesteryl ester, occurred in *CYP1A1/2* KO rats.

3.4. CYP1A1/2 deficiency promoted lipogenesis but inhibited lipid hydrolysis

The expression of lipogenesis related genes was detected through RT-qPCR in the *CYP1A1/2* KO rats. Our data show that *CYP1A1/2* deficiency significantly up-regulated SREBP1, SCD1 as well as the nuclear receptor LXRα in rat liver, thereby promoting cholesterol ester synthesis (Fig. 3A). However, the monoacylglycerol *O*-acyltransferase 1 (*Mogat1*, catalyzing the synthesis of diacylglycerols) was down-regulated (Fig. 3A), which may be responsible for the decrease of serum TG in KO rats. Fatty acid

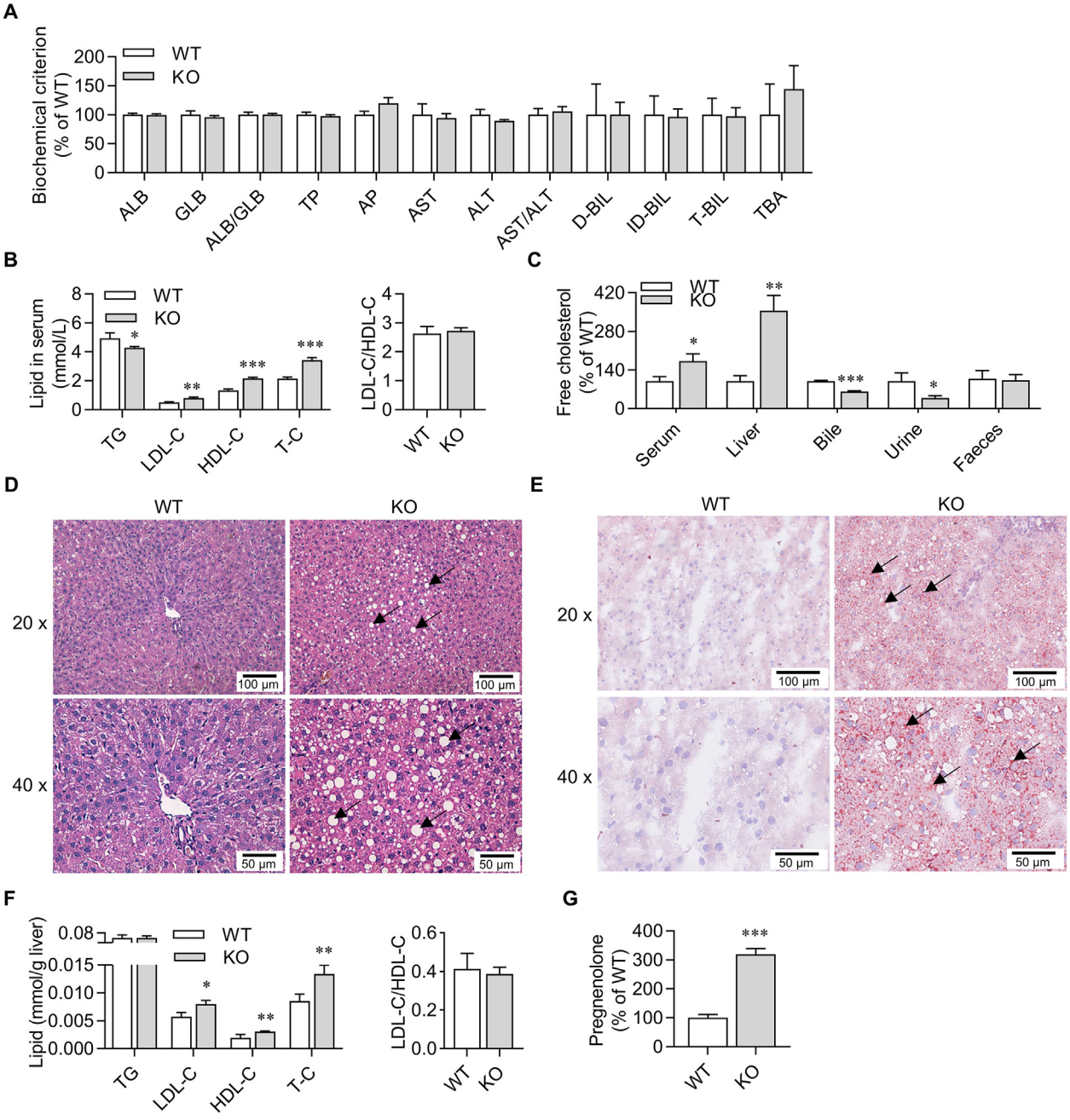

Figure 2 *CYP1A1/2* deficiency promoted cholesteryl ester accumulation. (A) Comparison of serum biochemical indexes between WT and KO rats. (B) Serum lipid content detection. (C) Comparison of free cholesterol concentration in the serum, liver, bile, urine and faeces between WT and KO rats. (D) Morphological analysis of liver tissues of *CYP1A1/2* KO rats using HE staining. (E) Lipid deposition in liver detection using oil red O staining. (F) Hepatic lipid content detection. (G) Detection of pregnenolone in serum. ALB, albumin; GLB, globulin; TP, total protein; AP, alkaline phosphatase; ALT, alanine aminotransferase; AST, aspartate aminotransferase; D-BIL, direct bilirubin; ID-BIL, indirect bilirubin; T-BIL, total, bilirubin; TBA, total bile acid; TG, triglyceride; LDL-C, low density lipoprotein-cholesterin; HLD-C, high density lipoprotein-cholesterin; T-C, total cholesterol. All data are expressed as mean ± SD, $n = 4$ in (A)−(C) and $n = 6$ in (F)−(G). $^{*}P < 0.05$, $^{**}P < 0.01$, $^{***}P < 0.001$, compared with data in the WT group.

synthase (*Fasn*), acyl-CoA cholesterol acyltransferase (*Acat*) and diacylglycerol *O*-acyltransferase (*Dgat*) remained unchanged in the liver of KO rats (Fig. 3A). The activation of LXRα−SREBP1−SCD1 pathway was confirmed in protein level by Western blot analysis (Fig. 3B).

The key enzymes of liver lipid hydrolysis in WT and KO rats were compared at mRNA levels. Down-regulation of most isoforms in the *Ces1* and *Ces2* family was observed in the liver of KO rats, and the downward trend of CES1 was confirmed at the protein level (Fig. 3C and D), while the CES2 protein remained unchanged (Fig. 3E). No significant differences in mRNA levels of hormone-sensitive lipase (*Hsl*), adipose triglyceride lipase (*Atgl*) and arylacetamide deacetylase (*Aada*) were observed between WT and *CYP1A1/2* KO rats (Fig. 3C).

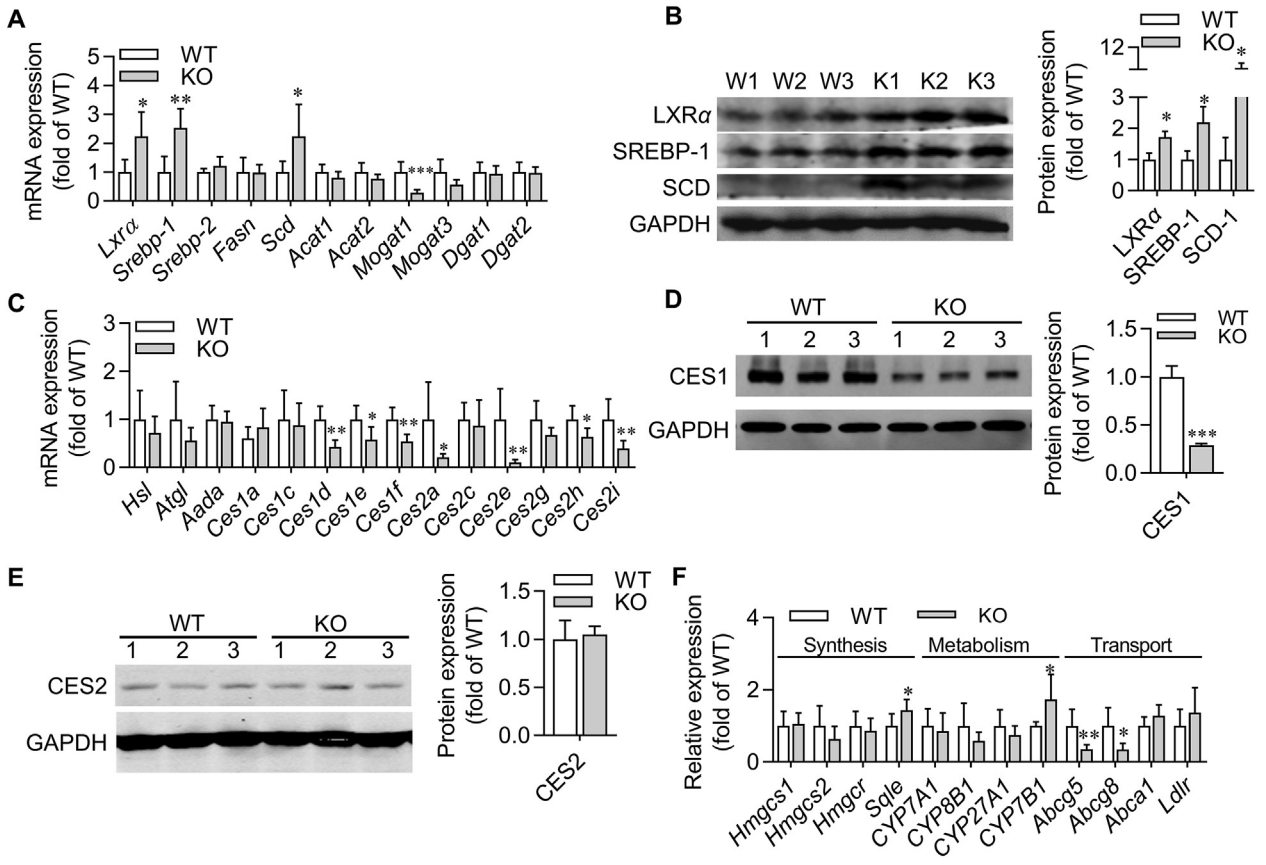

Figure 3 *CYP1A1/2* deficiency promoted lipogenesis but inhibited lipid hydrolysis. (A) mRNA expression of lipogenesis-related genes in the liver of *CYP1A1/2* KO rats. (B) Protein expression of lipogenesis-related genes in the liver of *CYP1A1/2* KO rats. (C) mRNA expression of genes involved in lipid hydrolysis in the liver of *CYP1A1/2* KO rats. (D) Protein expression of CES1 in the liver of *CYP1A1/2* KO rats. (E) Protein expression of CES2 in the liver of *CYP1A1/2* KO rats. (F) mRNA expression of genes involved in cholesterol synthesis, metabolism and transport in the liver of *CYP1A1/2* KO rats. All data are expressed as mean ± SD, $n = 6$ in (A) (C) (F) and $n = 3$ in (B) (D) (E). $^{*}P < 0.05$, $^{**}P < 0.01$, $^{***}P < 0.001$, compared with data in the WT group.

Cholesterol ester and the T-C in liver and serum of KO rats were significantly increased. Thus, the synthesis and metabolism of cholesterol in liver were explored. The 3-hydroxy-3-methylglutaryl-CoA synthase (*Hmgcs*), 3-hydroxy-3-methylglutaryl-CoA reductase (*Hmgcr*) and squalene epoxidase (*Sqle*) are crucial enzymes involved in the synthesis of cholesterol. The results showed that the mRNA level of *Sqle* was up-regulated by 40% in the liver of KO rats (Fig. 3F). Moreover, cholesterol can be metabolized into bile acids through classical and an alternative pathway, and CYP7A1, CYP8B1, CYP27A1 and CYP7B1 participate in the bio-transformation pathway[25]. Among these CYP isoforms, the mRNA expression of liver *CYP7B1* in KO rats increased by 70% (Fig. 3F). The efflux transporters such as *Abcg5*, *Abcg8* and *Abca 1* in the liver mediate the excretion of cholesterol from hepatocytes to the bile ducts, and ultimately promote the excretion of cholesterol from the body. *Ldlr* participates in the uptake of cholesterol from blood into hepatocytes. Our data show that the expression of *Abcg5* and *Abcg8* in the liver of KO rats decreased significantly (Fig. 3F). Lipid deposition in liver may affect fatty acid oxidation process. Therefore, the expression of related genes was also evaluated and compared. However, none of these tested genes was affected by *CYP1A1/2* deletion on the mRNA level (Supporting Information Fig. S4).

3.5. *CYP1A1/2 deficiency affected the distribution of bile acid subtypes*

Although there was no significant difference of the TBA content in the serum of WT and *CYP1A1/2* KO rats, the content and distribution of some bile acid subtypes in *CYP1A1/2* KO rats changed. The β-muricholic acid (β-MCA), cholic acid (CA), ursodeoxycholic acid (UDCA), chenodeoxycholic acid (CDCA) and deoxycholic acid (DCA) were detected in this study (Fig. 4). CA and CDCA were significantly increased in the serum of KO rats, while UDCA was decreased. In addition to DCA, other bile acid subtypes accumulated in the liver of *CYP1A1/2* KO rats, with different degrees. The concentrations of β-MCA, CA and UDCA in the bile of *CYP1A1/2* KO rats were lower than those of WT rats. However, β-MCA, CA and DCA were significantly increased in the faeces of *CYP1A1/2* KO rats, compared with those in WT rats.

3.6. *CYP1A induction reversed hepatic lipidosis in Ldlr KO rats*

In order to confirm the role of CYP1A in cholesterol accumulation, *Ldlr* KO rats were used to study the effect of CYP1A inducer on hepatic cholesterol deposition. We treated *Ldlr* KO rats with Lan for 3 weeks to induce the expression of CYP1A *in vivo*. Our

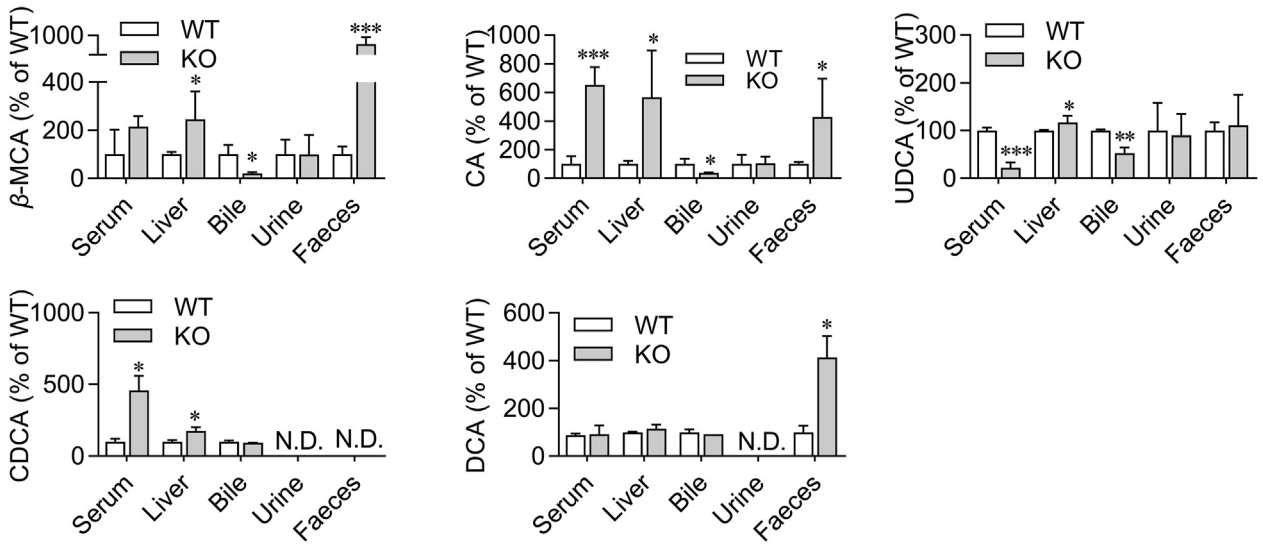

Figure 4 *CYP1A1/2* deficiency affected the distribution of bile acid subtypes. The β-muricholic acid (β-MCA), cholic acid (CA), ursodeoxycholic acid (UDCA), chenodeoxycholic acid (CDCA) and deoxycholic acid (DCA) were detected in the serum, liver, bile, urine and faeces of WT and *CYP1A1/2* KO rats. All data are expressed as mean ± SD, $n = 4$, $^{*}P < 0.05$, $^{**}P < 0.01$, $^{***}P < 0.001$, compared with data in the WT group.

data show that CYP1A protein expression was significantly induced after Lan treatment (Fig. 5A). HE staining presented that CYP1A induction significantly alleviated liver lipidosis in *Ldlr* KO rats (Fig. 5B). However, lipids in serum, including TG, LDL-C, HDL-C, and T-C, remained unchanged (Fig. 5C).

3.7. CYP1A induction reversed cholesterol deposition in the food-borne hypercholesteremia rat model

To further confirm the role of CYP1A in cholesterol accumulation, the effect of CYP1A inducer on cholesterol was studied in a food-borne hypercholesteremia rat model. After 11 weeks of HCD, the serum TG, LDL-C, and T-C contents in the solvent control group (HCD + Sol group) increased by 150%, 500% and 150%, respectively, compared with those of the LCD + Sol group. Moreover, the HDL-C/LDL-C ratio in the HCD + Sol group was 86% lower than that in the LCD + Sol group (Fig. 6A). These results indicate the food-borne hypercholesteremia model was successful constructed. However, compared with HCD + Sol group, the levels of serum TG, LDL-C, and T-C in the Lan treated group were significantly lower (Fig. 6A). The concentrations of TG decreased by 27% and 42%, after treatment with low dosage of Lan (10 mg/kg, HCD + Lan 10 group) and high dosage of Lan (50 mg/kg, HCD + Lan 50 group), respectively. Compared with the HCD + Sol group, LDL-C content decreased by 40% and 65%, respectively. Furthermore, compared with the HCD + Sol group, T-C content was reduced by 39% and 47%, respectively. More importantly, the HDL-C/LDL-C ratios in the HCD + Lan 10 group and HCD + Lan 50 group significantly increased by 170% and 200%, respectively, compared with that in the HCD + Sol group. Oil red O staining showed that the lipid accumulation in Lan treatment group (both 10 and 50 mg/kg group) was less than that in the HCD + Sol group (Fig. 6B). In addition to lipid deposition, the HCD feeding also causes severe liver injury, which is manifested by a significant increase in transaminases. However, Lan treatment reduced serum transaminases to physiological levels (Fig. 6C).

4. Discussion

In this study, *CYP1A1/2* KO rat model was firstly generated by CRISPR/Cas9, and successfully characterized by the loss of CYP1A protein expression and function. CYP1A is a relatively conserved P450 subfamily, and only two CYP1A isoforms (CYP1A1 and CYP1A2) have been reported. The cDNA sequences of *CYP1A1* and *CYP1A2* in rats are 83% and 80% similar to their corresponding subtypes in humans, respectively. It has been reported that KO of *CYP1A1* can promote the progression of nonalcoholic fatty liver induced by high-fat diet containing benzo[*a*]pyrene[21]. Pathological examination of the livers of *CYP1A2* KO mice revealed a 50% increase in lipid content in the interstitial cells of the KO mice[20]. These results show that the CYP1A subfamily plays a role in regulating lipid homeostasis, and suggest that CYP1A1 and CYP1A2 may have a synergistic effect in this process. Therefore, in order to simulate the complete deletion of CYP1A in rats *in vivo*, this study used CRISPR/Cas9 technology to construct double gene KO rats of *CYP1A1* and *CYP1A2* to study the role of CYP1A in cholesterol homeostasis.

It has been reported that CYP1A2 deficiency affects neonatal respiratory physiology and CYP1A2 is crucial for neonatal survival[19], which may explain the low birth rate and survival rate observed in our *CYP1A1/2* KO rats (Data not shown). This study demonstrated that systemic KO of *CYP1A1/2* can increase the accumulation of lipids in rats. Interestingly, compared with mice, the lipid accumulation in rat liver and serum was mainly cholesterol esters, not TG[20]. It is reported that the accumulation of free cholesterol in the liver may lead to cholesterol related steatohepatitis and play an important role in the development and progression of NASH[26]. Although there is no evidence that CYP1A is directly involved in cholesterol metabolism, it is reported that CYP1A is widely involved in the cholesterol metabolism network. For example, pregnenolone is an important intermediate in the CYP1A-related cholesterol metabolism pathway[11]. Our data show that pregnenolone was highly accumulated in the blood of KO

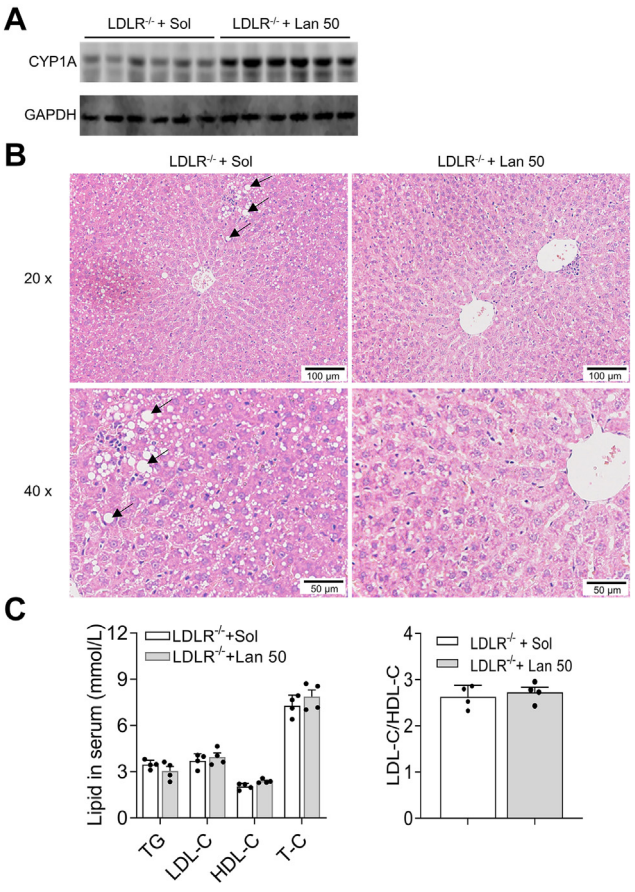

Figure 5 CYP1A induction reversed hepatic lipidosis of LDLR knockout rats. (A) Protein expression of CYP1A in the liver. (B) Morphological analysis of liver tissues using HE staining. (C) Serum lipid content detection. All data are expressed as mean ± SD, $n = 6$ in (A), $n = 4$ in (C).

rats. This may be the direct cause of cholesterol and cholesteryl ester accumulation in KO rats.

To further explore the impact of CYP1A deletion on lipid metabolism at the molecular level, we screened a series of lipid metabolism-related genes. Although the fatty acid oxidation pathway did not change, the lipogenesis pathway was overexpressed, and the lipid hydrolysis enzyme was down-regulated in the liver of *CYP1A1/2* KO rats. Increased cholesterol level can induce the transcriptional activity of LXR[27]. Therefore, cholesterol accumulation in *CYP1A1/2* KO rats promoted the transcription and expression of LXRα in the liver. Further, LXRα promotes the expression of transcriptional factor SREBP1, and SREBP1 finally induces SCD1 through binding to its promotor elements[28]. In addition, when SREBP1 is absent, LXRα can bind to the LXR responsive element on the *Scd1* promotor to induce the SCD1 expression directly[29,30]. SCD1 is the rate-limiting enzyme in the formation of monounsaturated fatty acids from saturated fatty acids, mainly catalyzing palmitoyl-CoA and stearoyl-CoA to produce palmitoleic acid and oleic acid, respectively. Then, the generated palmitoleic acid and oleic acid can be catalyzed to produce cholesteryl ester by *Acat* and TG through *Mgat* and *Dgat*[31]. In this study, the up-regulation of *Scd1* in the liver of *CYP1A1/2* KO rats may provide more precursors to produce cholesterol esters and TG, while the down-regulation of *Mgat1* reduces the production of TG, thus promoting the flow of lipid precursors to the formation of cholesterol ester. It is suggested that cholesterol accumulation can activate LXRα−SREBP1−SCD1 pathway in liver of *CYP1A1/2* KO rats, thus increasing the biosynthesis of cholesteryl ester. The potential mechanism of CYP1A-mediated cholesterol homeostasis is summarized in Fig. 7A.

CES1 possesses the activity of cholesteryl hydrolysis and is highly expressed in liver[32,33]. Meanwhile, the contents of cholesteryl ester in plasma and liver are increased in *Ces1* KO mouse model[34]. In this study, the expression of *Ces1* in the liver of *CYP1A1/2* KO rats was down-regulated, which may promote the deposition of cholesterol ester in plasma and liver. Although cholesterol has no inhibitory effect on CES1, its metabolites, especially 27-hydroxycholesterol, have a strong selective inhibitory effect on CES1[35,36]. Hence, cholesterol accumulation in *CYP1A1/2* KO rats may increase the concentration of 27-hydroxycholesterol, eventually leading to the specific inhibition of CES1 in the liver of KO rats. To further explore the regulation of CES1 in the *CYP1A1/2 KO* rats, we measured the mRNA expression of a series of reported potential regulators of CES1, such as CAR, Nrf 2 and HGF. However, no significant difference was detected between WT and KO rats (Data not shown).

Additionally, the up-regulation of *Sqle* in the liver of *CYP1A1/2* KO rats also increased the synthesis of cholesterol. Although CYP7B1, an enzyme involved in the alternative pathway of cholesterol-bile acid transformation, was up-regulated by 70% in the KO rat liver, no significant difference was detected in the TBA. Interestingly, the content of some cholic acid subtypes such as CA and CDCA increased in the serum and liver of *CYP1A1/2* KO rats, while the content of UDCA in the serum of *CYP1A1/2* KO rats was dramatically decreased. The inconsistency of changes in the content of various bile acid subtypes in *CYP1A1/2* KO rats may be the reason for the unchanged TBA concentration. Different bile acids in turn affect cholesterol homeostasis. UDCA is a hydrophilic bile acid that has been used to treat gallstones[37,38]. UDCA administration reduces cholesterol concentration in bile by reducing the output of liver cholesterol[39,40]. There are also reports that β-MCA can prevent diet-induced cholesterol gallstones and promote the dissolution of cholesterol gallstones in mice[41].

To further verify the role of CYP1A in cholesterol deposition, the rat model of hypercholesteremia was treated with CYP1A inducer. Lan, a proton pump inhibitor, is a typical strong CYP1A inducer in rats both *in vitro* and *in vivo*[42]. It has been reported that Lan administration (50 mg/kg/day) for 7 days can increase the metabolic activity of CYP1A in rats by 4 times[42]. Therefore, in order to ensure the induction effect, the high dose of 50 mg/kg/day was used in this study. Moreover, the clinical dose of Lan is 60 mg/kg/day, and the equivalent dose in rats is about 6 mg/kg/day[43]. Therefore, the dose of 10 mg/kg/day closing to clinical dosage was also used in this study.

LDLR deficiency in humans is related to increased T-C in plasma, resulting in higher risk of hypercholesterolemia[44]. Therefore, *Ldlr* KO rat model was applied to explore the therapeutic effect of Lan on hypercholesterolemia. Surprisingly, the lipid deposition in the liver of *Ldlr* KO rats were significantly reduced, but the plasma cholesterol content remained unchanged. Liver is the main organ to remove LDL from the circulation, and *Ldlr* mediates the endocytosis of cholesterol by hepatocytes to maintain the level of LDL in blood[45]. Thus, the way that LDL enters hepatocytes through endocytosis is blocked in *Ldlr* KO rats. We speculate that CYP1A can only effectively remove lipids in

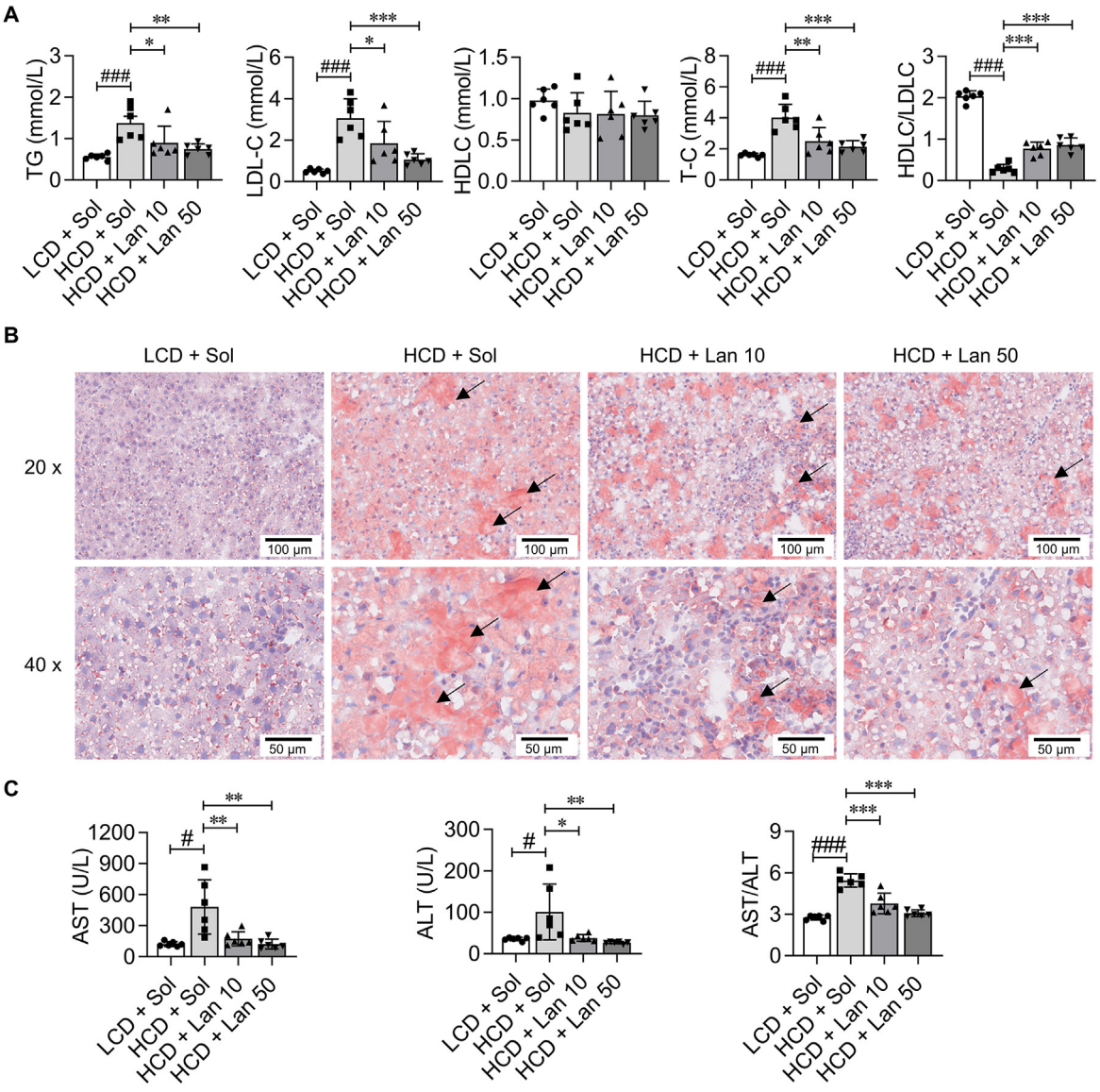

Figure 6 CYP1A induction reversed cholesterol accumulation in the food-borne hyperlipidemia model. (A) Serum lipid content detection. (B) Morphological analysis of liver tissues using oil red O staining. (C) Serum transaminase content detection. All data are expressed as mean ± SD, $n = 6$ for each group. $^{\#}P < 0.05$, $^{\#\#\#}P < 0.01$, compared with data in the LCD + Sol group. $^{*}P < 0.05$, $^{**}P < 0.01$, $^{***}P < 0.001$, compared with data in the HCD + Sol group.

the liver of *Ldlr* KO rats, because CYP1A is mainly expressed in the liver and the main route of LDL transport from the blood to the liver is missing in *Ldlr* KO rats. Therefore, a food-borne hypercholesteremia rat model was further used to explore the therapeutic effect of Lan on hypercholesterolemia. In this model, Lan treatment not only significantly reduced the cholesterol deposition in the liver, but also significantly reduced the blood cholesterol content of rats, suggesting that CYP1A inducer has therapeutic effects on food-borne hypercholesteremia. In order to exclude the effects of on the stomach and food intake/nutrient absorption, the energy intakes of different groups of rats were also calculated and compared. Our results show that there was no significant difference in the energy consumption of each group during the experiments (data not shown). This study is the first time to reveal the cholesterol lowering effect of lansoprazole, which provides some basic research for the development of new functions of lansoprazole. Since CYP1A is a classic drug metabolizing enzyme, previous studies on CYP1A mainly focus on the metabolism of exogenous substances, including drug metabolism, drug interactions, and compound toxicity[46,47]. In contrast, the physiological or pathological effects of CYP1A based on endogenous metabolism are rarely reported. The *CYP1A1/2* KO rat model provides a good tool for studying the physiological functions mediated by CYP1A. Especially in the research of lipid metabolism-related diseases, rats not only have the characteristics of large size and more body fluids, but also possess disease phenotypes more similar to humans[44,48].

By searching the gnomAD database, a total of 707 SNPs of *CYP1A1* was found, of which 49% (346/707) SNPs were missense mutations. For *CYP1A2*, 780 SNPs were found and 46% (357/780) of them were missense mutations. The above mutation sites were screened by pathogenicity scoring software (SIFT<0.05,

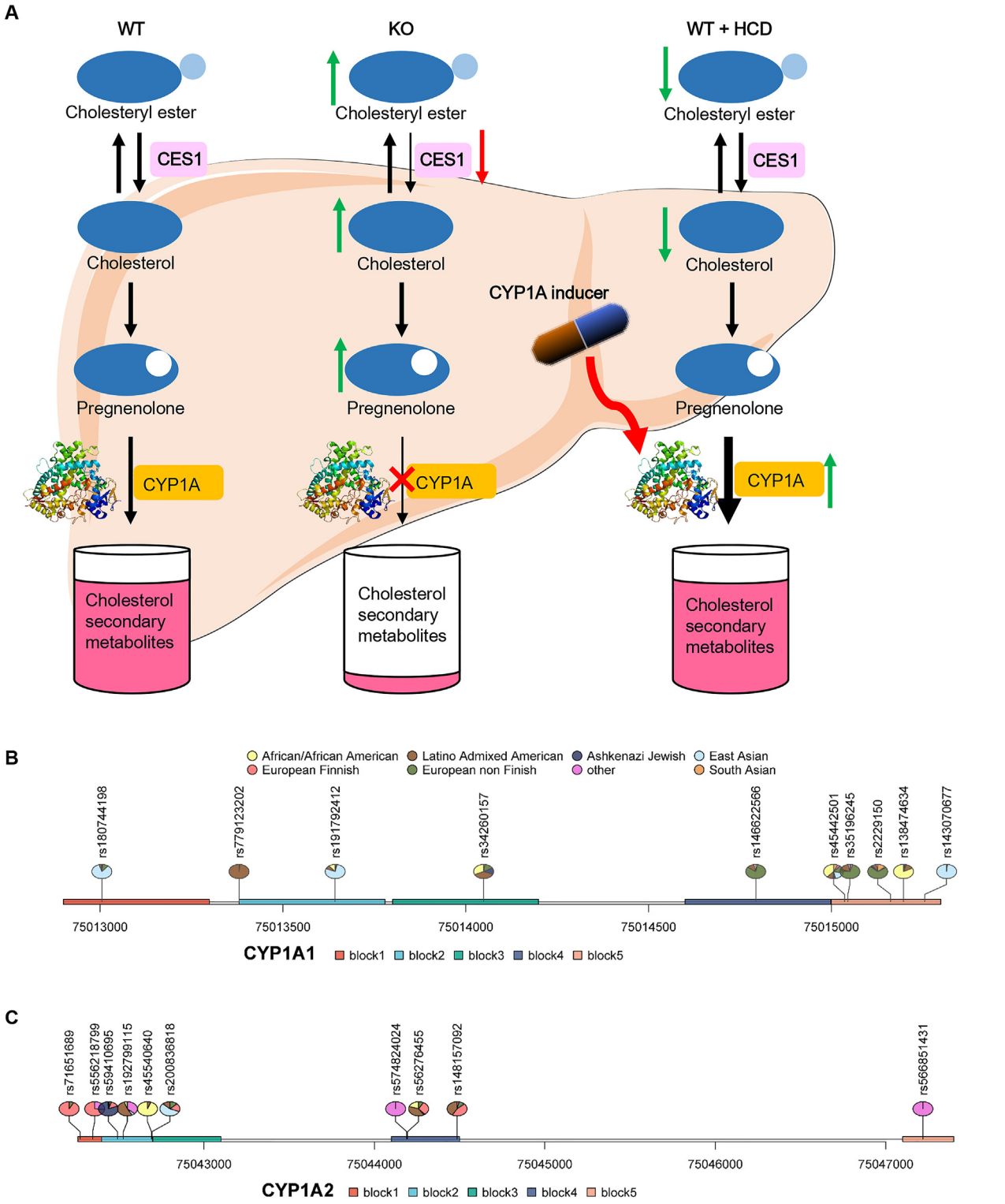

Figure 7 Potential mechanism of CYP1A-mediated cholesterol homeostasis maintenance and potential risk SNPs of *CYP1A1* and *CYP1A2* in gnomAD. (A) In WT rats, CYP1A is widely involved in the bio-transformation network of cholesterol, and pregnenolone is an important intermediate in the CYP1A-related cholesterol metabolism pathway. In *CYP1A1/2* KO rats, pregnenolone was accumulated, leading to the increase of cholesterol. In the food-borne hyperlipidemia rat model, CYP1A inducer reversed the phenotype of lipidosis. Black arrow, flow direction of material transformation; Green arrow, increased content of the substance or increased expression of the gene; Straight red arrow, decreased expression of the gene. (B) Population distribution of main *CYP1A1* SNPs. (C) Population distribution of main *CYP1A2* SNPs. Through searching the gnomAD database, 707 and 780 SNPs of *CYP1A1* and *CYP1A2* were found, respectively. All mutation sites were screened by pathogenicity scoring software (SIFT<0.05, CADD>20, Polyphen2_HVAR_score>0.9 and M-CAP<0.95), and some clinically reported benign mutations were also excluded. Finally, 130 and 124 highly pathogenic mutations of *CYP1A1* and *CYP1A2* were obtained. The population distribution of the top 10 highly pathogenic mutations (mutation frequency) was analyzed.

CADD>20, Polyphen2_HVAR_score>0.9 and M-CAP<0.95), and the benign mutations reported in clinic were excluded. Finally, 130 and 124 highly pathogenic mutations of *CYP1A1* and *CYP1A2* were obtained. The population distribution of the top ten highly pathogenic mutations (mutation frequency) was further analyzed. For *CYP1A1*, the East Asian population mainly contains SNPs such as rs180744198, rs191792412 and rs143070677, while the Latino Admixed American population mainly possesses SNP of rs779123202 (Fig. 7B). For *CYP1A2*, the Ashkenazi Jewish population mainly has the mutation of rs59410695, while the African/African American population primarily contains SNP of rs45540640 (Fig. 7C). The above data indicate that there are differences in the population distribution of these pathogenic mutations. By searching the GWAS Catlog database, we also found that some SNPs of *CYP1A1* and *CYP1A2* in humans were related to CVD such as coronary heart disease and hypertension[49,50], suggesting that human *CYP1A* mutations may be a risk factor for CVD.

In addition, we are committed to finding direct clinical evidence to support or verify the results we observed in rats. Through the bioinformatics method, we hope to find enough data about the population with loss-of-function mutations on *CYP1A1/2*, calculate the frequency of occurrence of hyperlipidemia or hypercholesterolemia in these people, and analyze the expression of *CYP1A1/2* in this population. However, the results of the database (gnomad) showed that the allele frequencies of loss-of-function SNPs of both *CYP1A1* and *CYP1A2* were very low in the population. For example, the allele frequencies of rs180744198 (SNP of *CYP1A1*) and rs45540640 (SNP of *CYP1A2*) in the population were 0.0004631 and 0.0004525, respectively (Supporting Information Fig. S5). Therefore, there are not enough reported expression data for reference among cholesterolemia patients with WT and *CYP1A1/2* SNPs. We also analyzed the expression of *CYP1A1* and *CYP1A2* in hypercholesterolemia population using data from GEO datasets. Our results show that there was no significant difference in the expression of *CYP1A1* and *CYP1A2* between the control group and the hypercholesterolemic group (Supporting Information Fig. S6). This may be due to two reasons. First, the absence or low expression of CYP1A1/2 may be a cause rather than a consequence of hypercholesterolemia, so the changes in CYP1A1/2 expression cannot be detected in patients with familial hypercholesterolemia (usually driven by mutations in other genes). Secondly, the number of valid samples is limited, and the results can not reflect the actual situation.

Although we have not found sufficient clinical evidence to confirm the role of *CYP1A1/2* in humans at present, this study still has important scientific significance. First, from an evolutionary point of view, the low-frequency mutations that exist in the population may be some gene mutations that currently have no practical role in the population, and are in a low-frequency state because they cannot be enriched. It is also possible that some highly deleterious mutations are difficult to enrich in the population, although they produce phenotypes that are detrimental to the population. For *CYP1A1/2*, by searching the GWAS Catlog database, we found that some SNPs of *CYP1A1* and *CYP1A2* in humans were related to CVD such as coronary heart disease and hypertension. At the same time, our animal experiments also proved that the deletion of *CYP1A1/2* could cause the accumulation of cholesteryl esters in rats. Combined with the conserved characteristics of *CYP1A1/2* gene sequences between rats and humans, we have reason to infer that the low-frequency loss-of-function mutation of *CYP1A1/2* in the population may be caused by the adverse phenotype after its mutation. Secondly, there is currently no direct evidence that loss-of-function mutations in *CYP1A1/2* in the population are drivers of hypercholesterolemia. However, one method worth studying is to treat or alleviate the accumulation of cholesterol or cholesterol esters by inducing *CYP1A1/2*. In fact, the results of our animal experiments also confirmed the feasibility of this idea in rats.

5. Conclusions

CYP1A1/2 deletion in rats obstructed the metabolic network of cholesterol, leading to the accumulation of cholesterol and cholesteryl ester. On the one hand, the increase of cholesterol content activated LXRα−SREBP1−SCD1 pathway and promoted the lipogenesis. On the other hand, the accumulation of cholesterol may also contribute to the inhibition of CES1, thus finally increasing the deposition of cholesteryl esters. Importantly, CYP1A induction could reverse cholesterol deposition in rat models of hypercholesteremia. This study found the important role of CYP1A in cholesterol homeostasis, which provides a new perspective for the treatment of hypercholesterolemia.

Acknowledgments

This work was supported in whole or part by grants from the National Natural Science Foundation of China (81773808, 82274010), the Science and Technology Commission of Shanghai Municipality (18430760400, China), the Jointed PI Program from Shanghai Changning Maternity and Infant Health Hospital (2019CNECNUPI02, China), the Fundamental Research Funds for the Central Universities (China), and ECNU Construction Fund of Innovation and Entrepreneurship Laboratory (China). This work was also supported from ECNU Multifunctional Platform for Innovation (011, China) and the Instruments Sharing Platform of School of Life Sciences, East China Normal University (Shanghai, China).

Author contributions

Jian Lu and Xin Wang designed the experiments. Jian Lu, Xuyang Shang, Dongyi Sun, and Jie Liu performed the experiments and collected data. Jian Lu, Bingyi Yao, Yuanjin Zhang, He Wang, and Jingru Shi analyzed the data. Jian Lu, Xuyang Shang, Bingyi Yao, Jie Liu, and Yuanjin Zhang drafted the manuscript. Xin Wang supervised the study. Huaqing Chen provided the LDLR KO rat model. Tieliu Shi, Mingyao Liu, and Xin Wang reviewed and revised the manuscript.

Conflicts of interest

The authors declare no conflicts of interest.

Appendix A. Supporting information

Supporting data to this article can be found online at https://doi.org/10.1016/j.apsb.2022.08.005.

References

1. Xiao C, Dash S, Morgantini C, Hegele RA, Lewis GF. Pharmacological targeting of the atherogenic dyslipidemia complex: the next

frontier in CVD prevention beyond lowering LDL cholesterol. *Diabetes* 2016;**65**:1767−78.
2. El-Tantawy WH, Temraz A. Natural products for controlling hyperlipidemia: review. *Arch Physiol Biochem* 2019;**125**:128−35.
3. Xie Z, Zhang M, Song Q, Cheng L, Zhang X, Song G, et al. Development of the novel ACLY inhibitor 326E as a promising treatment for hypercholesterolemia. *Acta Pharm Sin B* 2022. Available from: https://doi.org/10.1016/j.apsb.2022.06.011.
4. Luo J, Yang H, Song BL. Mechanisms and regulation of cholesterol homeostasis. *Nat Rev Mol Cell Biol* 2020;**21**:225−45.
5. Rezen T, Rozman D, Pascussi JM, Monostory K. Interplay between cholesterol and drug metabolism. *Biochim Biophys Acta* 2011;**1814**:146−60.
6. Okerson T, Patel J, DiMario S, Burton T, Seare J, Harrison DJ. Effect of 2013 ACC/AHA Blood Cholesterol Guidelines on statin treatment patterns and low-density lipoprotein cholesterol in atherosclerotic cardiovascular disease patients. *J Am Heart Assoc* 2017;**6**:e004909.
7. Virani SS, Alonso A, Benjamin EJ, Bittencourt MS, Callaway CW, Carson AP, et al. Heart disease and stroke statistics—2020 update: a report from the American Heart Association. *Circulation* 2020;**141**:e139−596.
8. Centers for Disease C, Prevention. Vital signs: prevalence, treatment, and control of high levels of low-density lipoprotein cholesterol—-United States, 1999−2002 and 2005−200. *MMWR Morb Mortal Wkly Rep* 2011;**60**:109−14.
9. Zhao D, Liu J, Wang M, Zhang X, Zhou M. Epidemiology of cardiovascular disease in China: current features and implications. *Nat Rev Cardiol* 2019;**16**:203−12.
10. Wang HH, Garruti G, Liu M, Portincasa P, Wang DQ. Cholesterol and lipoprotein metabolism and atherosclerosis: recent advances in reverse cholesterol transport. *Ann Hepatol* 2017;**16**:s27−42.
11. Lu J, Shang X, Zhong W, Xu Y, Shi R, Wang X. New insights of CYP1A in endogenous metabolism: a focus on single nucleotide polymorphisms and diseases. *Acta Pharm Sin B* 2020;**10**:91−104.
12. Rizzolo D, Kong B, Taylor RE, Brinker A, Goedken M, Buckley B, et al. Bile acid homeostasis in female mice deficient in *Cyp7a1* and *Cyp27a1*. *Acta Pharm Sin B* 2021;**11**:3847−56.
13. Chambers KF, Day PE, Aboufarrag HT, Kroon PA. Polyphenol effects on cholesterol metabolism *via* bile acid biosynthesis, CYP7A1: a review. *Nutrients* 2019;**11**:2588.
14. Lan X, Yan J, Ren J, Zhong B, Li J, Li Y, et al. A novel long noncoding RNA Lnc-HC binds hnRNPA2B1 to regulate expressions of Cyp7a1 and Abca 1 in hepatocytic cholesterol metabolism. *Hepatology* 2016;**64**:58−72.
15. Rizzolo D, Buckley K, Kong B, Zhan L, Shen J, Stofan M, et al. Bile acid homeostasis in a cholesterol 7 alpha-hydroxylase and sterol 27-hydroxylase double knockout mouse model. *Hepatology* 2019;**70**:389−402.
16. Nelson ER, Wardell SE, Jasper JS, Park S, Suchindran S, Howe MK, et al. 27-Hydroxycholesterol links hypercholesterolemia and breast cancer pathophysiology. *Science* 2013;**342**:1094−8.
17. Nebert DW, Russell DW. Clinical importance of the cytochromes P450. *Lancet* 2002;**360**:1155−62.
18. Stading R, Chu C, Couroucli X, Lingappan K, Moorthy B. Molecular role of cytochrome P4501A enzymes inoxidative stress. *Curr Opin Toxicol* 2020;**20**−**21**:77−84.
19. Pineau T, Fernandez-Salguero P, Lee SS, McPhail T, Ward JM, Gonzalez FJ. Neonatal lethality associated with respiratory distress in mice lacking cytochrome P450 1A2. *Proc Natl Acad Sci U S A* 1995;**92**:5134−8.
20. Smith AG, Davies R, Dalton TP, Miller ML, Judah D, Riley J, et al. Intrinsic hepatic phenotype associated with the *Cyp1a2* gene as shown by cDNA expression microarray analysis of the knockout mouse. *EHP Toxicogenomics* 2003;**111**:45−51.
21. Uno S, Nebert DW, Makishima M. Cytochrome P450 1A1 (CYP1A1) protects against nonalcoholic fatty liver disease caused by Western diet containing benzo[*a*]pyrene in mice. *Food Chem Toxicol* 2018;**113**:73−82.
22. Li D, Qiu Z, Shao Y, Chen Y, Guan Y, Liu M, et al. Heritable gene targeting in the mouse and rat using a CRISPR-Cas system. *Nat Biotechnol* 2013;**31**:681−3.
23. Lu J, Shao Y, Qin X, Liu D, Chen A, Li D, et al. CRISPR knockout rat cytochrome P450 3A1/2 model for advancing drug metabolism and pharmacokinetics research. *Sci Rep* 2017;**7**:42922.
24. Wang X, Lee WY, Or PM, Yeung JH. Effects of major tanshinones isolated from Danshen (*Salvia miltiorrhiza*) on rat CYP1A2 expression and metabolism of model CYP1A2 probe substrates. *Phytomedicine* 2009;**16**:712−25.
25. Hashimoto M, Kobayashi K, Watanabe M, Kazuki Y, Takehara S, Inaba A, et al. Knockout of mouse *Cyp3a* gene enhances synthesis of cholesterol and bile acid in the liver. *J Lipid Res* 2013;**54**:2060−8.
26. Horn CL, Morales AL, Savard C, Farrell GC, Ioannou GN. Role of cholesterol-associated steatohepatitis in the development of NASH. *Hepatol Commun* 2022;**6**:12−35.
27. Wang B, Tontonoz P. Liver X receptors in lipid signalling and membrane homeostasis. *Nat Rev Endocrinol* 2018;**14**:452−63.
28. Miyazaki M, Dobrzyn A, Man WC, Chu K, Sampath H, Kim HJ, et al. Stearoyl-CoA desaturase 1 gene expression is necessary for fructose-mediated induction of lipogenic gene expression by sterol regulatory element-binding protein-1c-dependent and -independent mechanisms. *J Biol Chem* 2004;**279**:25164−71.
29. Chu K, Miyazaki M, Man WC, Ntambi JM. Stearoyl-coenzyme A desaturase 1 deficiency protects against hypertriglyceridemia and increases plasma high-density lipoprotein cholesterol induced by liver X receptor activation. *Mol Cell Biol* 2006;**26**:6786−98.
30. Rahman SM, Janssen RC, Choudhury M, Baquero KC, Aikens RM, de la Houssaye BA, et al. CCAAT/enhancer-binding protein beta (C/EBPbeta) expression regulates dietary-induced inflammation in macrophages and adipose tissue in mice. *J Biol Chem* 2012;**287**:34349−60.
31. Paton CM, Ntambi JM. Biochemical and physiological function of stearoyl-CoA desaturase. *Am J Physiol Endocrinol Metab* 2009;**297**:E28−37.
32. Xu J, Li Y, Chen WD, Xu Y, Yin L, Ge X, et al. Hepatic carboxylesterase 1 is essential for both normal and farnesoid X receptor-controlled lipid homeostasis. *Hepatology* 2014;**59**:1761−71.
33. Wang D, Zou L, Jin Q, Hou J, Ge G, Yang L. Human carboxylesterases: a comprehensive review. *Acta Pharm Sin B* 2018;**8**:699−712.
34. Quiroga AD, Li L, Trotzmuller M, Nelson R, Proctor SD, Kofeler H, et al. Deficiency of carboxylesterase 1/esterase-x results in obesity, hepatic steatosis, and hyperlipidemia. *Hepatology* 2012;**56**:2188−98.
35. Crow JA, Herring KL, Xie S, Borazjani A, Potter PM, Ross MK. Inhibition of carboxylesterase activity of THP1 monocytes/macrophages and recombinant human carboxylesterase 1 by oxysterols and fatty acids. *Biochim Biophys Acta* 2010;**1801**:31−41.
36. Mangum LC, Hou X, Borazjani A, Lee JH, Ross MK, Crow JA. Silencing carboxylesterase 1 in human THP-1 macrophages perturbs genes regulated by PPARgamma/RXR and RAR/RXR: down-regulation of CYP27A1−LXRalpha signaling. *Biochem J* 2018;**475**:621−42.
37. Wang HH, Portincasa P, de Bari O, Liu KJ, Garruti G, Neuschwander-Tetri BA, et al. Prevention of cholesterol gallstones by inhibiting hepatic biosynthesis and intestinal absorption of cholesterol. *Eur J Clin Invest* 2013;**43**:413−26.
38. Ridlon JM, Bajaj JS. The human gut sterolbiome: bile acid-microbiome endocrine aspects and therapeutics. *Acta Pharm Sin B* 2015;**5**:99−105.
39. Einarsson K. Effect of ursodeoxycholic acid on hepatic cholesterol metabolism. *Scand J Gastroenterol Suppl* 1994;**204**:19−23.
40. Guan B, Tong J, Hao H, Yang Z, Chen K, Xu H, et al. Bile acid coordinates microbiota homeostasis and systemic immunometabolism in cardiometabolic diseases. *Acta Pharm Sin B* 2022;**12**:2129−49.
41. Wang DQ, Tazuma S. Effect of beta-muricholic acid on the prevention and dissolution of cholesterol gallstones in C57L/J mice. *J Lipid Res* 2002;**43**:1960−8.

42. Masubuchi N, Hakusui H, Okazaki O. Effects of pantoprazole on xenobiotic metabolizing enzymes in rat liver microsomes: a comparison with other proton pump inhibitors. *Drug Metab Dispos* 1997;**25**:584−9.
43. Ogawa R, Echizen H. Drug−drug interaction profiles of proton pump inhibitors. *Clin Pharmacokinet* 2010;**49**:509−33.
44. Zhao Y, Yang Y, Xing R, Cui X, Xiao Y, Xie L, et al. Hyperlipidemia induces typical atherosclerosis development in *Ldlr* and *Apoe* deficient rats. *Atherosclerosis* 2018;**271**:26−35.
45. He Y, Rodrigues RM, Wang X, Seo W, Ma J, Hwang S, et al. Neutrophil-to-hepatocyte communication *via* LDLR-dependent miR-223-enriched extracellular vesicle transfer ameliorates nonalcoholic steatohepatitis. *J Clin Invest* 2020:141513.
46. Zhou SF, Wang B, Yang LP, Liu JP. Structure, function, regulation and polymorphism and the clinical significance of human cytochrome P450 1A2. *Drug Metab Rev* 2010;**42**:268−354.
47. Jin Q, Wu J, Wu Y, Li H, Finel M, Wang D, et al. Optical substrates for drug-metabolizing enzymes: recent advances and future perspectives. *Acta Pharm Sin B* 2022;**12**:1068−99.
48. Iannaccone PM, Jacob HJ. Rats. *Dis Model Mech* 2009;**2**:206−10.
49. Kichaev G, Bhatia G, Loh PR, Gazal S, Burch K, Freund MK, et al. Leveraging polygenic functional enrichment to improve GWAS power. *Am J Hum Genet* 2019;**104**:65−75.
50. German CA, Sinsheimer JS, Klimentidis YC, Zhou H, Zhou JJ. Ordered multinomial regression for genetic association analysis of ordinal phenotypes at Biobank scale. *Genet Epidemiol* 2020;**44**:248−60.